

See discussions, stats, and author profiles for this publication at: <https://www.researchgate.net/publication/26818364>

Red- and Green-Emitting Iridium(III) Complexes for a Dual Barometric and Temperature-Sensitive Paint

ARTICLE in CHEMISTRY - A EUROPEAN JOURNAL · SEPTEMBER 2009

Impact Factor: 5.73 · DOI: 10.1002/chem.200901511 · Source: PubMed

CITATIONS

51

READS

102

6 AUTHORS, INCLUDING:



[Lorenz H Fischer](#)

Universität Regensburg

16 PUBLICATIONS 772 CITATIONS

SEE PROFILE



[Matthias I J Stich](#)

PreSens - Precision Sensing GmbH

22 PUBLICATIONS 746 CITATIONS

SEE PROFILE



[Elisabeth Holder](#)

Bergische Universität Wuppertal

58 PUBLICATIONS 1,979 CITATIONS

SEE PROFILE



[Michael Schaeferling](#)

Bundesanstalt für Materialforschung und -...

77 PUBLICATIONS 1,933 CITATIONS

SEE PROFILE

Red- and Green-Emitting Iridium(III) Complexes for a Dual Barometric and Temperature-Sensitive Paint

Lorenz H. Fischer,^[a] Matthias I. J. Stich,^[a] Otto S. Wolfbeis,^[a] Nan Tian,^[b, c]
Elisabeth Holder,^{*[b, c]} and Michael Schäferling^{*[a]}

Abstract: A new dual luminescent sensitive paint for barometric pressure and temperature (T) is presented. The green-emitting iridium(III) complex $[\text{Ir}(\text{ppy})_2(\text{carbac})]$ (ppy = 2-phenylpyridine; carbac = 1-(9*H*-carbazol-9-yl)-5,5-dimethylhexane-2,4-dione) was applied as a novel probe for T along with the red-emitting complex $[\text{Ir}(\text{btpy})_3]$, (btpy = 2-(benzo[*b*]thiophene-2-yl)pyridine) which functions as a barometric (in fact oxygen-sensitive) probe. Both iridium complexes were dissolved in different polymer materials to achieve optimal responses. The probe $[\text{Ir}(\text{ppy})_2(\text{carbac})]$ was dispersed in gas-blocking

poly(acrylonitrile) microparticles in order to suppress any quenching of its luminescence by oxygen. The barometric probe $[\text{Ir}(\text{btpy})_3]$, in turn, was incorporated in a cellulose acetate butyrate film which exhibits good permeability for oxygen. The effects of temperature on the response of the oxygen probe can be corrected by simultaneous optical determination of T , as the poly(acrylonitrile) microparticles containing

Keywords: dyes/pigments • imaging agents • iridium • luminescence • sensors

the temperature indicator are incorporated into the film. The phosphorescent signals of the probes for T and barometric pressure, respectively, can be separated by optical filters due to the ≈ 75 nm difference in their emission maxima. The dual sensor is applicable to luminescence lifetime imaging of T and barometric pressure. It is the first luminescent dual sensor material for barometric pressure/ T based exclusively on the use of Ir^{III} complexes in combination with luminescence lifetime imaging.

Introduction

The determination of oxygen partial pressure (and of air pressure in general) is of great interest in a variety of medical, biological, and technical applications. Both can be mea-

sured by using luminescent oxygen-sensitive materials.^[1–5] Such materials change their luminescence intensities and lifetimes depending on the oxygen partial pressure. Luminescent probes for oxygen are usually incorporated in a gas-permeable polymer matrix, and can be applied in various formats such as sensor foils or fiber optic sensors.^[6–8] The measurement of barometric pressure plays an essential role in aerodynamics and in fluid mechanics.^[9,10]

Barometric pressure can be imaged with a luminescent oxygen-sensitive coating, often referred to as a pressure sensitive paint (PSP). Imaging offers a spatial resolution unsurpassed by any other method for the determination of barometric pressure, and PSPs, unlike other sensors, do not disturb the gas flow in wind tunnels. However, luminescent probes for barometric pressure are sensitive to temperature as well. It has therefore been suggested that, by analogy to PSPs, a temperature indicator should be incorporated into a similar sensor layer in order to measure T (a so-called temperature-sensitive paint, TSP), or in order to correct for the effect of T on the response of the PSP. TSPs use gas-blocking matrix polymers in order to avoid the quenching of luminescence by oxygen.^[11,12] The relationship between poly-

[a] L. H. Fischer, M. I. J. Stich, Prof. O. S. Wolfbeis, Dr. M. Schäferling
Institute of Analytical Chemistry
Chemo- and Biosensors, University Regensburg
Universitätsstr. 93051 Regensburg (Germany)
Fax: (+49) 941-943-4064
E-mail: michael.schaeferling@chemie.uni-regensburg.de

[b] N. Tian, Prof. E. Holder
Functional Polymers Group and Institute of Polymer Technology
University of Wuppertal
Gaußstr. 20, 42097 Wuppertal (Germany)
Fax: (+49) 202-439-3880
E-mail: holder@uni-wuppertal.de

[c] N. Tian, Prof. E. Holder
Dutch Polymer Institute (DPI)
P.O. Box 513, 5600 AX Eindhoven (The Netherlands)

mer structure, oxygen permeation and diffusion in the polymer, and oxygen quenching efficiencies has been reviewed by Lu et al.^[8] Finally, dual PSP/TSP sensors have been reported^[13–15] based on the possibility of optical sensors to give several signals simultaneously (in this case one for barometric pressure and one for T), which can be separated by optical filters provided the probes emit at sufficiently different wavelengths and with insignificant spectral overlap, or if the decay times of the luminescence lifetimes differ by a certain amount.^[16]

Several problems that occur in sensing based on measurement of luminescence intensity can be overcome by making use of time-resolved gated lifetime detection. In detail, lifetime imaging is insensitive towards variations in thickness of the sensor layer, inhomogeneous sample surface and illumination, reflections and scatter of excitation light, photobleaching of fluorescent probes and leaching of the dyes, and interferences by strong ambient light.^[17] Luminescence lifetime imaging is an intrinsically referenced method that is not influenced by varying distances between sample and detector, nor by applying different detectors or excitation light sources.^[18] A typical measurement is performed by using LEDs or laser diodes as the excitation light sources, and by detecting the luminescence by means of a CCD camera. Luminescence lifetime imaging is often performed by the rapid lifetime determination (RLD) method.^[19] Thereby, the probe is excited by a short pulse of light, and the luminescence intensity emitted from the sensor layer is gathered by the CCD camera in two precisely timed gates.

Here, we report on the preparation and calibration of a dual sensor for barometric pressure and T , which consists of two organometallic iridium(III) probes dissolved in appropriate “binder” polymers. Various organometallic complexes have been used so far as indicator probes in PSPs and TSPs. Principally, Pt^{II} and Pd^{II} porphyrins and porpholactones have been employed as probes for sensing barometric pressure, because their luminescence is strongly quenched by oxygen even in polymer solution.^[20–24] Complexes of Eu^{III} and Ru^{II} have been presented for use in sensing T .^[25,26] Iridium(III) probes, in contrast, have not been widely investigated with respect to their suitability for sensing oxygen or barometric pressure^[1,27–31] and, until now, they have not been employed for the purposes of sensing T even though they display bright and tunable emission colors and phosphorescence lifetimes in the range 1–10 μ s,^[32–35] which makes them perfectly suited for lifetime imaging applications.

Results

Sensor composition: The dual sensor material consists of the green-emitting temperature probe di(2-phenylpyridinato-C₂,N){1-(9H-carbazol-9-yl)-5,5-dimethylhexane-2,4-dione}-iridium(III), [Ir(ppy)₂(carbac)], and the red-emitting oxygen probe tris[2-(benzo[b]thiophene-2-yl)pyridinato-C₃,N]iridium(III), [Ir(btpy)₃]. The temperature-sensitive probe [Ir(ppy)₂(carbac)] was applied in gas-blocking poly(acryl-

onitrile) (PAN) microparticles with a diameter of about 1 μ m prepared by precipitation.

These [Ir(ppy)₂(carbac)]/PAN microparticles were dispersed in a solution of cellulose acetate butyrate (CAB), and the oxygen probe [Ir(btpy)₃] in THF. This “cocktail” was spread on a solid poly(ethylene terephthalate) (PET) support by knife coating. After evaporation of the solvent, the one-layer sensor was obtained with optical response to either temperature (T) or barometric pressure (p).

The thickness of the sensor film was approximately 6 μ m. The cross section of the sensor device and the chemical structures of the fluorophores are depicted in Figure 1. The

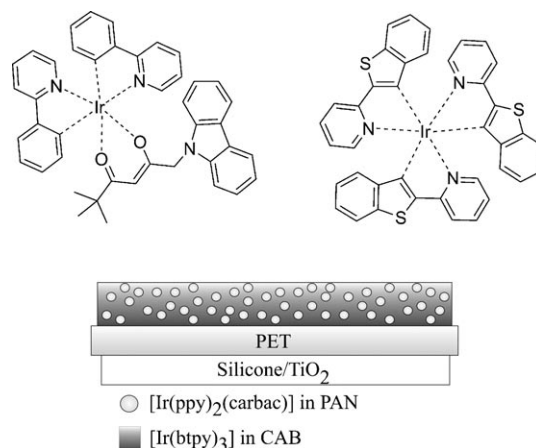


Figure 1. Top: Structures of the indicators Left: temperature indicator [Ir(ppy)₂(carbac)].^[33] Right: oxygen indicator [Ir(btpy)₃]. Bottom: Scheme of the dual sensitive sensor layer. The CAB film is cast on a PET support by knife-coating. It contains the probe for barometric pressure (in fact for oxygen). The microparticles made of PAN doped with the temperature probe are dispersed in the CAB film. The bottom side of the PET layer is coated with a highly reflective silicone/TiO₂ screen layer in order to improve optical readout, which is performed from the top.

bottom of the substrate foil was coated with a highly reflective 100 μ m TiO₂/silicone screen-layer. PAN has a very low gas permeability^[36] (P is 0.00015×10^{-13} cm³ (STP) cm (cm²sPa)^{−1}, STP=standard temperature and pressure). It shields the temperature probe from undesired oxygen quenching.

The dual sensor layer was cast from a 5% solution (w/w) of CAB in THF doped with [Ir(btpy)₃] and [Ir(ppy)₂(carbac)]. The permeability of the polymer hosting the oxygen probe is one of the major factors governing the quenching of the luminescence of the fluorophore. In this case, the sensor material was optimized for determination of air pressures up to 1500 mbar. Almost all established probes for luminescent barometric sensors are quenched to a wide extent at atmospheric pressure, which makes them useful only for pressures up to 1 bar. CAB was found to be a suitable polymer, with an oxygen permeability^[36] of 3.56×10^{-13} cm³ (STP) cm (cm²sPa)^{−1}.

Signal separation: Table 1 shows the UV/Vis absorption and emission maxima, decomposition temperatures (T_d), and lu-

Table 1. UV/Vis absorption and emission maxima of 10 μm chloroform solutions, decomposition temperatures (T_d), and luminescence lifetimes (τ) of the iridium(III) complexes.

Compound	Absorbance [nm] (log ϵ , [mol $^{-1}$ dm 3 cm $^{-1}$])	Emission maximum [nm]	T_d [°C]	Lifetime ^[a] τ [μs]
[Ir(ppy) $_2$ (carbac)]	270 (4.71), 342 (4.06), 408 (3.58), 459 (3.45)	521	337 ^[b]	3.65
[Ir(btpy) $_3$]	292 (4.83), 366 (4.31), 408 (4.34)	596, 645	465 ^[b]	8.60

[a] At 50 mbar air pressure and 1 °C. [b] At 5 % weight loss.

minescence lifetimes (τ) of the iridium(III) complexes. The emission of the luminescence of [Ir(ppy) $_2$ (carbac)] peaks at 521 nm, and that of [Ir(btpy) $_3$] at 596 nm. As the emission band of [Ir(ppy) $_2$ (carbac)] is fairly narrow, the two signals can be almost quantitatively separated by optical filters, as

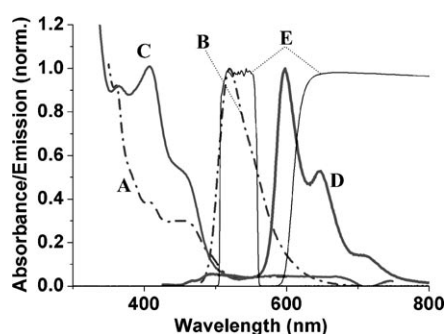


Figure 2. Optical spectra of the sensor system. A) Absorbance and B) emission of [Ir(ppy) $_2$ (carbac)]. C) Absorbance and D) emission of [Ir(btpy) $_3$]. E) Transmittance of the optical filters employed (BP 530/50 and RG 610).

shown in Figure 2. The emission of [Ir(ppy) $_2$ (carbac)] was optically isolated from other light using a BP 530/50 band-pass filter (530 nm indicating the center wavelength, 50 indicating the spectral bandpass). The oxygen-sensitive emission of [Ir(btpy) $_3$] was separated by an RG 610 longpass filter. This minimizes interference by the emission of the temperature probe, although at the expense of the intensity of the pressure signal.

The single pressure-sensitive film was then investigated in more detail using a fiber optic spectrometer. Emission spectra were acquired at different pressures at 24 °C. Figure 3 displays the pressure dependency of the emission spectrum of [Ir(btpy) $_3$], and shows that all maxima are quenched with

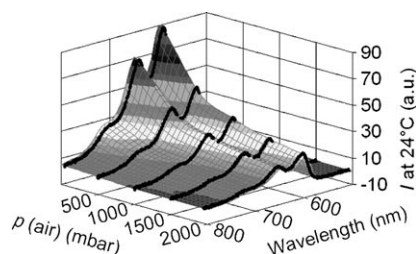


Figure 3. 3D intensity (I) plot of the pressure dependency of the emission spectra of the single pressure sensor [Ir(btpy) $_3$] in 6 μm CAB film at 24 °C.

equal efficiency. The emission spectrum of the temperature probe has one maximum only. Its temperature dependence is given in Figure 4. The dynamic range covers the range of highest practical interest (0 to > 50 °C).

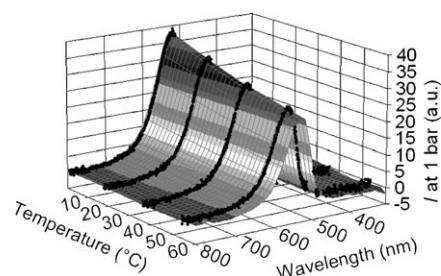


Figure 4. 3D intensity (I) plot of the temperature dependency of the emission spectra of the single temperature sensor [Ir(ppy) $_2$ (carbac)] in 6 μm PAN film at 24 °C.

Calibration of the dual sensor: The calibration of the sensor was performed by time-gated lifetime imaging using the RLD method.^[18,37] Thereby, the decay of the luminescence intensity is considered to be monoexponential, allowing a simple calculation of the luminescence lifetimes. Furthermore, the intrinsic reference accomplished by calculating an intensity ratio of two gates severely reduces the signal noise. The decay times of the phosphorescence of the metal–ligand complexes described here are in the range 2.5–8 μs . Rather than using large (or expensive) lasers, we prefer to use small and inexpensive LED light sources for photoexcitation. The intensity of luminescence is measured in two precisely timed gates by a triggered CCD camera, followed by a dark image for background subtraction (see Figure 5). After the light

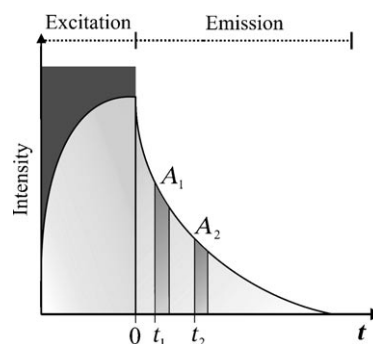


Figure 5. Scheme of the RLD method. A_1 and A_2 are the integrated intensities acquired by the CCD camera within the two precisely timed gates.

pulse has decayed, luminescence intensity is acquired in the first gate. This is repeated several times over a certain period of time (the integration time) and the measured intensities are accumulated and displayed as the first image. Afterwards, the second gate and the dark image are recorded likewise.

The integration time has to be carefully chosen because it defines, for example, the overall intensities of the images taken. The complete RLD acquisition process typically takes three times the integration time. The RLD imaging parameters are summarized in Table 2.

Table 2. Basic settings for luminescence lifetime imaging according to the RLD scheme displayed in Figure 7.

	Excitation [μs]	Gate width [μs]	t_1 [μs]	t_2 [μs]	Integration time [ms]
[Ir(ppy) ₂ (carbac)] (T)	5	1.4	0	0.7	150
[Ir(btpy) ₃] (p)	5	1	0	0.5	265

The intensity values (A_1 , A_2 in Figure 5) can be used to estimate the luminescence lifetimes (τ) according to Equation (1).^[11]

$$\tau = \frac{t_2 - t_1}{\ln A_1/A_2} \quad (1)$$

This equation reflects correct lifetimes only if 1) both time gates have the same width and 2) the decays are mono-exponential. The latter is not the case for both probes applied here, so the calculated lifetimes cannot be considered to be exact. There are, however, two good reasons to use the RLD method: firstly, it is a fast method that is hardly affected by the usual interferences in intensity measurements; secondly, we are not interested in exact lifetime values, but rather in their relative change to obtain an intrinsically referenced optical signal. In addition, the results are highly reproducible and are not adversely affected by variations in the intensity of the excitation light.

The sensing layer (with a sensing area of 3×3 cm) was mounted inside the calibration chamber. It can be calibrated at barometric pressures ranging from 50 to 2000 mbar. The temperature was adjusted using a Peltier element from 1 to 55°C. The wavelength of the excitation light was 405 nm throughout all measurements.

The phosphorescence intensity and lifetime decrease with rising temperature. This is also referred to as thermal quenching.^[11] The results of the temperature calibration from 1–54°C are shown in Figure 6. The T -sensitive probe displayed almost no cross-sensitivity towards barometric pressure in the range from 50 to 1950 mbar. The pressure dependency of the temperature probe is displayed in Figure 7. Unlike other temperature sensors,^[3,38,39] its calibration plot is linear over a rather wide temperature range, with a correlation coefficient R^2 of 0.999. The temperature coefficient of the decay time is 0.42 % °C⁻¹. There are various temperature sensors for imaging applications described

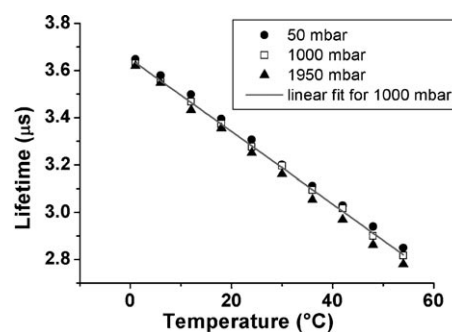


Figure 6. Temperature dependency of the luminescence lifetime of [Ir(ppy)₂(carbac)] in PAN microparticles with linear fit for 1000 mbar air pressure.

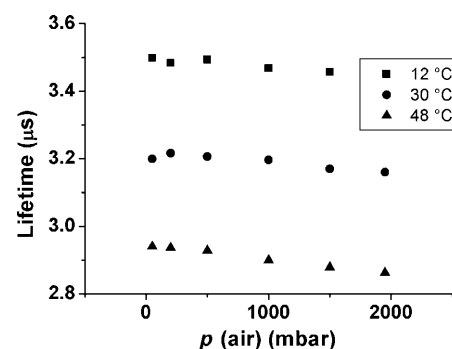


Figure 7. Pressure dependency of the luminescence lifetime of [Ir(ppy)₂(carbac)] in PAN microparticles.

in the literature, for example based on Eu^{III} or Ru^{II} complexes^[3,4,38] with somewhat higher temperature coefficients, but these also display much higher cross-sensitivities towards oxygen.

The quenching of the lifetime and the intensity of the luminescence of the oxygen probe Ir(btpy)₃ is due to collisional quenching by oxygen, and can be described by the Stern–Volmer equation. The deviation from linearity is described by the so called “two-site model”, as given in Equation (2), in which I and I_0 are the intensity of luminescence and τ and τ_0 are the corresponding lifetimes with and without quencher, respectively; f_1 and f_2 are the emissive fractions; K_{SV}^1 and K_{SV}^2 are the Stern–Volmer constants and $[Q]$ is the quencher concentration.^[11]

$$\frac{I}{I_0} = \frac{\tau}{\tau_0} = \frac{f_1}{1 + K_{SV}^1[Q]} + \frac{f_2}{1 + K_{SV}^2[Q]} \quad (2)$$

Figure 8 gives lifetime calibration plots at various temperatures. Such plots do not reveal whether quenching follows Stern–Volmer (SV) kinetics. Therefore, SV plots were generated as shown in Figure 9. The standard deviation of the lifetimes (<4%) is not really significant. The SV constants and correlation coefficients (R^2) are summarized in Table 3.

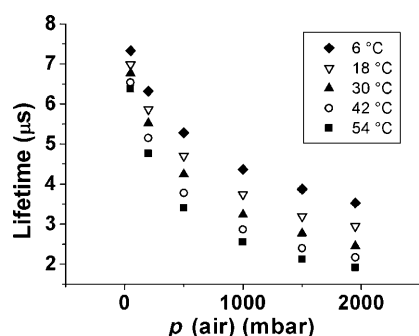


Figure 8. Pressure dependency at various temperatures of the phosphorescence lifetime of $[\text{Ir}(\text{btpy})_3]$ dissolved in a CAB film (thickness 6 μm).

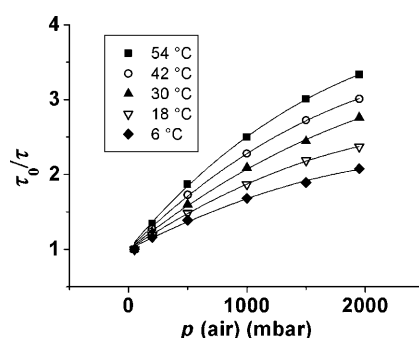


Figure 9. Stern-Volmer plots of the quenching by oxygen (expressed as air pressure) of the emission of $[\text{Ir}(\text{btpy})_3]$ dissolved in CAB polymer at various temperatures.

Table 3. Stern-Volmer constants (K_{SV}) of the quenching of the luminescence of $[\text{Ir}(\text{btpy})_3]$ in CAB calculated from the fits in Figure 9 according to the two-site model. Fitting parameters were set to $f_1=0.9$ and $f_2=0.1$.

T [$^{\circ}\text{C}$]	K_{SV}^1 [10^{-4} mbar $^{-1}$]	K_{SV}^2 [10^{-4} mbar $^{-1}$]	R^2
54	21.2 ± 0.9	-1.0 ± 0.3	0.997
42	17.6 ± 0.7	-1.1 ± 0.3	0.997
30	14.2 ± 0.6	-1.0 ± 0.3	0.997
18	11.7 ± 0.4	-1.6 ± 0.2	0.998
6	9 ± 0.8	-1.8 ± 0.3	0.996

Discussion

The metal-ligand complex (MLC) $[\text{Ir}(\text{ppy})_2(\text{carbac})]$ is found to be a very useful luminescent probe for T . Dissolved in polyacrylonitrile polymer, its luminescence lifetime linearly responds over a large range and displays a remarkably low cross-sensitivity towards oxygen. Although several probes for T described previously^[3,4,38] have higher temperature coefficients, these also suffer from a much stronger cross-sensitivity to oxygen or barometric pressure. The fairly narrow emission band of $[\text{Ir}(\text{ppy})_2(\text{carbac})]$ peaks at 521 nm, and this facilitates its spectral separation from the luminescence of the oxygen-sensitive probe emitting in the deep red. The $[\text{Ir}(\text{btpy})_3]$ complex is shown to be a viable probe for oxygen and barometric pressure. Dissolved in the polymer CAB it covers a pressure range from 0 to 2000 mbar or higher. It is possible to reduce the cross-sensitivity of this probe towards T by employing fluoroacrylic matrix poly-

mers like FIB,^[18,23] albeit at the expense of a smaller dynamic range.^[4] Established oxygen probes such as $\text{Pt}[5,10,15,20\text{-tetra-(pentafluorophenyl) porphyrin}]$ (PtTFPP)^[3,38] are more sensitive to oxygen, but have distinctly smaller dynamic ranges when used in comparable matrix polymers. The dynamic range of PtTFPP may be extended to about 1000 mbar barometric pressure by applying less permeable matrices, but then its temperature dependence becomes distinctly higher^[3] compared to the $[\text{Ir}(\text{btpy})_3]/\text{CAB}$ sensor system.

Conclusion

A novel dual p (air)/ T sensor system has been prepared. It consists of two different iridium complexes as luminescent indicators. These indicators are incorporated into two different polymer matrices, thus controlling the dynamic range and the sensitivity, and avoiding interferences. The sensor was calibrated using the RLD method for imaging. The signals for barometric pressure and temperature can be separated by optical filters. The homogeneity of the sensor layer, along with the benefits of the intrinsically referenced lifetime imaging, provides highly reproducible, accurate, and simultaneous determination of barometric pressure and temperature at a very high spatial resolution. The results obtained at the calibration of this new sensor system are very promising for its future applications in fluid mechanics as a dual one-layer PSP/TSP.

Experimental Section

Materials: All synthesis procedures were performed under an atmosphere of dry argon by employing usual Schlenk techniques. Solvents were carefully dried and distilled from appropriate drying agents prior to use. Commercially available reagents were used without further purification unless otherwise stated. 2-Phenylpyridine, N,N -dimethylformamide, tetrahydrofuran, tris[2-(benzo[*b*]thiophene-2-yl)pyridinato- C^3N]iridium(III) $[\text{Ir}(\text{btpy})_3]$, poly(vinyl alcohol), cellulose acetobutylate (CAB), and titanium dioxide were purchased from Sigma-Aldrich (www.sigmaaldrich.com). $\text{IrCl}_3 \cdot n\text{H}_2\text{O}$, 2-ethoxyethanol and pinacolone were purchased from ABCR (www.abcr.de). Ethyl bromoacetate, sodium hydride, and 9H-carbazole were purchased from Acros (www.acros.com). Poly(acrylonitrile) was purchased from Polysciences (www.polysciences.com), Elastosil A07 silicone from Wacker (www.wacker.com), and PET foil (Mylar[®]) from Goodfellow (www.goodfellow.com).

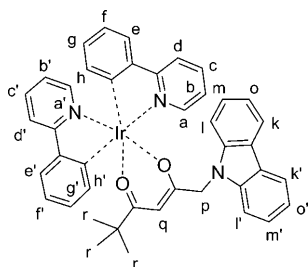
Instrumentation and methods: ^1H NMR and ^{13}C NMR spectra were acquired on a Bruker ARX 400, (www.bruker.com) chemical shifts are given relative to the internal standard tetramethylsilane (Me_4Si) in CDCl_3 . Chemical shifts in NMR spectra are given in ppm and coupling constants in Hz (s=singlet, d=doublet, t=triplet, q=quartet, and m=multiplet). Fourier transform infrared (FTIR) spectra were recorded on a Jasco FT/IR-4200 Fourier transform spectrometer (www.jasco.de). The UV/Vis spectra were measured with a JASCO V-550 UV/Vis spectrophotometer (www.jasco.de; 1 cm cuvettes, CHCl_3) at concentrations of about 1×10^{-5} mol L^{-1} . The emission spectra were performed using a CARY Eclipse fluorescence spectrophotometer (www.varianinc.com) at concentrations of about 1×10^{-5} mol L^{-1} . Thermogravimetric analysis (TGA) was performed on a Mettler Toledo TGA/DSC STAR System (www.mettler-toledo.de; heating rate: 10 K min^{-1} ; argon; T_d @5% weight loss). Mass spectra were obtained using a Varian MAT 311 instrument (www.varia-

nine.com) with an electrospray source (ESIMS), a Voyager-DE PRO Biospectrometry (www.appliedbiosystems.com); MALDI-TOF) and a micro-TOF instrument from Bruker Daltonik (Bremen, Germany; www.bruker.de) equipped with a multi-purpose ion source (MPIS) made by the machine shop at the University of Wuppertal. In this case atmospheric pressure laser ionization method was used as ionization technique.^[40,41] Elemental analyses (EA) were performed on a Perkin-Elmer 240B setup.

Synthetic methods

Synthesis of $[\text{Ir}^{\text{III}}(\text{ppy})_2\text{Cl}]_2$: The synthesis of the precursor complex $[\text{Ir}^{\text{III}}(\text{ppy})_2\text{Cl}]_2$ followed well-described procedures published elsewhere in literature.^[33,42,43] Spectral characterization: ^1H NMR (400 MHz, CDCl_3 , 25 °C, TMS): δ = 5.86 (d, $^3J(\text{H,H})$ = 7.9 Hz, 2H), 6.59 (t, $^3J(\text{H,H})$ = 7.0 Hz, 2H), 6.74–6.97 (m, 4H), 7.54 (d, $^3J(\text{H,H})$ = 7.0 Hz, 2H), 7.72–7.86 (m, 2H), 7.92 (d, $^3J(\text{H,H})$ = 7.9 Hz, 2H), 9.24 ppm (d, $^3J(\text{H,H})$ = 6.2 Hz, 2H); MALDI-TOFMS: m/z : calcd for $\text{C}_{44}\text{H}_{32}\text{Cl}_2\text{Ir}_2\text{N}_4$: 1072; found: 1073.

Synthesis of $[\text{Ir}^{\text{III}}(\text{ppy})_2[1-(9H\text{-carbazol-9-yl})-5,5\text{-dimethylhexane-2,4-dione}]]$:^[33] This was accomplished in essence by analogy to the procedure given in reference [33]. The precursor (200 mg, 0.187 mmol), the carbac ligand^[33] (115 mg, 0.373 mmol), and potassium carbonate (180 mg, 1.306 mmol) were dissolved with 2-ethoxyethanol (30 mL) in a 50 mL flask, and the mixture was stirred under reflux for 3 h. After cooling to room temperature, 2-ethoxyethanol was removed under reduced pressure. The crude product was dissolved in dichloromethane (20 mL) and the solid was filtered off. The solution was concentrated under reduced pressure and the residue was purified by silica column chromatography (*n*-hexane/ethyl acetate, 10/3 v/v) to give a green powder. Yield: (175 mg, 58 %); ^1H NMR (400 MHz, CDCl_3 , 25 °C, TMS): δ = 0.57^f (s, 9H), 4.53–4.73^p (q, 2H), 5.05^q (s, 1H), 6.26–6.28^h (d, $^3J(\text{H,H})$ = 7.6 Hz, 1H), 6.37–6.39^h (d, $^3J(\text{H,H})$ = 7.6 Hz, 1H), 6.64–6.80^g (t, $^3J(\text{H,H})$ = 8.1 and 7.6 Hz, 1H), 6.71–6.75^g (t, $^3J(\text{H,H})$ = 7.1 and 7.6 Hz, 1H), 6.77–6.81^f (t, $^3J(\text{H,H})$ = 7.1 and 7.6 Hz, 1H), 6.85–6.88^f (t, $^3J(\text{H,H})$ = 7.1 and 8.1 Hz, 1H), 6.90–6.94^b (t, $^3J(\text{H,H})$ = 5.6 and 7.6 Hz, 1H), 6.97–7.00^b (t, $^3J(\text{H,H})$ = 5.6 and 8.1 Hz, 1H), 7.21–7.26^{m,m',o,o'} (m, 4H), 7.32–7.36^{j,l} (m, 2H), 7.49–7.51^{c'} (d, $^3J(\text{H,H})$ = 7.6 Hz, 1H), 7.58–7.60^e (d, $^3J(\text{H,H})$ = 7.6 Hz, 1H), 7.63–7.67^c (t, $^3J(\text{H,H})$ = 7.6 and 8.1 Hz, 1H), 7.70–7.74^c (t, $^3J(\text{H,H})$ = 7.6 and 8.7 Hz, 1H), 7.76–7.78^d (d, $^3J(\text{H,H})$ = 8.1 Hz, 1H), 7.84–7.86^d (d, $^3J(\text{H,H})$ = 8.1 Hz, 1H), 8.06–8.08^{k,k'} (d, $^3J(\text{H,H})$ = 7.6 Hz, 2H), 8.27–8.28^a (d, $^3J(\text{H,H})$ = 5.6 Hz, 1H), 8.39–8.40^p ppm (d, $^3J(\text{H,H})$ = 5.1 Hz, 1H); ^{13}C NMR (400 MHz, CDCl_3 , 25 °C, TMS): δ = 27.5, 40.9, 51.5, 92.2, 109.1, 117.9, 118.3, 119.0, 120.1, 120.4, 120.7, 120.9, 121.2, 123.0, 123.5, 123.8, 125.6, 128.7, 129.1, 133.2, 133.6, 136.7, 140.7, 144.7, 144.8, 147.6, 147.8, 148.1, 148.2, 168.5, 168.7, 180.9, 196.5 ppm; IR (KBr): $\tilde{\nu}$ = 3039 (C–H), 2989, 2957 (C–H), 1679, 1567 (C=C, C=N, C=O), 1467, 1434, 876, 858, 790, 738, 717, 689, 654 cm^{-1} ; UV/Vis (CHCl_3): λ_{max} (log ϵ) = 261 (5.99), 345 (5.37), 410 (4.84), 453 nm ($4.71 \text{ mol}^{-1} \text{ dm}^3 \text{ cm}^{-1}$); emission (CHCl_3): λ_{max} = 521 nm; TGA: T_d (@ 5 % weight loss) = 337 °C; APLI-MS: m/z : calcd for $\text{C}_{42}\text{H}_{36}\text{IrN}_3\text{O}_2$: 807; found: 807; elemental analysis calcd (%) for $\text{C}_{42}\text{H}_{36}\text{IrN}_3\text{O}_2$: C 62.51, H 4.50, N 5.21; found: C 62.34, H 4.73, N 5.53.



Synthesis of PAN micro-particles containing $[\text{Ir}(\text{ppy})_2(\text{carbac})]$: PAN (200 mg) was dissolved in *N,N*-dimethylformamide (DMF) (40 mL). After the polymer was fully dissolved, $[\text{Ir}(\text{ppy})_2(\text{carbac})]$ (7 mg) was added to the solution. Double distilled water (140 mL) was added dropwise under vigorous stirring of the solution. The precipitated microparti-

cles were centrifuged and washed with water four times. They were then dispersed in double distilled water and were subsequently freeze-dried. Prior to use in the dual sensor, the microparticles were washed three times with ethanol and three times with THF, dispersed in double distilled water and freeze-dried again.

Experimental setup for sensor calibration: Absorption and emission spectra were recorded on a Lambda 14p Perkin-Elmer UV/Vis spectrophotometer (Waltham, MA, USA, www.perkinelmer.com) and an Aminco AB 2 luminescence spectrometer (Thermo Scientific Inc., Waltham, MA, USA, www.thermo.com), respectively. The *p/T* calibration chamber was provided by the German Aerospace Center (DLR) in Göttingen. All time-resolved measurements were performed with a PCO SensiCam 12 bit b/w CCD camera (PCO, Kelheim, Germany, www.pco.de) equipped with a Schneider-Kreuznach Xenon 0.95/17 lens (Jos. Schneider Optische Werke, Bad Kreuznach, Germany, www.schneiderkreuznach.com) and a 405–66–60 405 nm LED from Roithner Lasertechnik (Vienna, Austria, www.roithner-laser.com). The excitation light was focused by a PCX 18 18 MgF2 TS lens from Edmund Optics (Karlsruhe, Germany, www.edmundoptics.com). It was filtered through a BG 12 filter (Schott, Mainz, Germany, www.schott.com) with a thickness of 2 mm. Emission was detected through a BP 530/50 band pass filter and an RG 610 high pass filter, purchased from AHF Analysentechnik (www.ahf.de).

Acknowledgements

E.H. and M.S. both acknowledge the Deutsche Forschungsgemeinschaft (DFG) for financial support. This research forms part of the research program of the Dutch Polymer Institute (DPI), project #629. We thank Dr. Ulrich Henne and Dr. Christian Klein from the German Aerospace Center (DLR) in Göttingen for providing the calibration unit. E.H. acknowledges Prof. Ullrich Scherf for granting access to the tools of the Macromolecular Chemistry at the University of Wuppertal (BUW) and Anke Helfer for TGA analysis; Melanie Dausend and Jürgen Döneck (Organic Chemistry, BUW) for performing routine mass spectrometry, and Oliver Schmitz and Ralf Schieweg (Analytical Chemistry, BUW) for performing APLI-MS measurements, as well as Ralf Radon (Analytical Chemistry, BUW) for elemental analysis.

- [1] Y. Amao, Y. Ishikawa, I. Okura, *Anal. Chim. Acta* **2001**, *445*, 177–182.
- [2] K. Mitsuo, K. Asai, A. Takahashi, H. Mizushima, *Meas. Sci. Technol.* **2006**, *17*, 1282.
- [3] M. I. Stich, S. Nagl, O. S. Wolfbeis, U. Henne, M. Schaeferling, *Adv. Funct. Mater.* **2008**, *18*, 1399–1406.
- [4] B. Zelelew, G. E. Khalil, G. Phelan, B. Carlson, M. Gouterman, J. B. Callis, L. R. Dalton, *Sens. Actuators B* **2003**, *96*, 304–314.
- [5] G. E. Khalil, A. Chang, M. Gouterman, J. B. Callis, L. R. Dalton, N. J. Turro, S. Jockusch, *Rev. Sci. Instrum.* **2005**, *76*, 054101–1–8.
- [6] J. I. Peterson, R. V. Fitzgerald, *Anal. Chem.* **1984**, *56*, 62–67.
- [7] G. B. Hocker, *Appl. Opt.* **1979**, *18*, 1445–1448.
- [8] X. Lu, I. Manners, M. A. Winnik in *New Trends in Fluorescence Spectroscopy*, (Eds.: B. Valeur, J.-C. Brochon), Springer, Berlin, **2001**, pp. 229–254.
- [9] J. W. Holmes, *J. Fluoresc.* **1993**, *3*, 179–183.
- [10] R. H. Engler, C. Klein, O. Trinks, *Meas. Sci. Technol.* **2000**, *11*, 1077–1085.
- [11] J. H. Bell, E. T. Schairer, L. A. Hand, R. D. Mehta, *Annu. Rev. Fluid Mech.* **2001**, *33*, 155–206.
- [12] M. A. Woodmansee, J. C. Dutton, *Exp. Fluids* **1998**, *24*, 163–174.
- [13] J. Hradil, C. Davis, K. Mongey, C. McDonagh, B. D. MacCraith, *Meas. Sci. Technol.* **2002**, *13*, 1552–1557.
- [14] K. Nakakita, M. Kurita, K. Mitsuo, S. Watanabe, *Meas. Sci. Technol.* **2006**, *17*, 359–366.
- [15] M. Kameda, N. Tezuka, T. Hangai, K. Asai, K. Nakakita, Y. Amao, *Meas. Sci. Technol.* **2004**, *15*, 489–500.

- [16] S. Nagl, O. S. Wolfbeis, *Analyst* **2007**, *132*, 507–511.
- [17] M. E. Lippitsch, J. Pusterhofer, M. J. P. Leiner, O. S. Wolfbeis, *Anal. Chim. Acta* **1988**, *205*, 1–6.
- [18] M. I. Stich, O. S. Wolfbeis, *Fluorescence Sensing and Imaging Using Pressure-Sensitive Paints and Temperature-Sensitive Paints*, Springer, Heidelberg, **2008**.
- [19] R. J. Woods, S. Scypinski, Love, L. J. Cline, H. A. Ashwoth, *Anal. Chem.* **1984**, *56*, 1395–1400.
- [20] S.-K. Lee, I. Okura, *Anal. Sci.* **1997**, *13*, 535–540.
- [21] S.-K. Lee, I. Okura, *Spectrochim. Acta Part A* **1998**, *54*, 91–100.
- [22] P. M. Gewehr, D. T. Delpy, *Med. Biol. Eng. Comput.* **1993**, *31*, 11–21.
- [23] E. Puklin, B. Carlson, S. Gouin, *J. Appl. Polym. Sci.* **1999**, *71*, 2795–2804.
- [24] R. C. Evans, P. Douglas, J. A. G. Williams, D. L. Rochester, *J. Fluoresc.* **2006**, *16*, 201–206.
- [25] M. Gouterman, J. Callis, L. Dalton, G. E. Khalil, Y. M'ebarki, *Meas. Sci. Technol.* **2004**, *15*, 1986–1994.
- [26] S. Grenoble, M. Gouterman, G. E. Khalil, *J. Lumin.* **2005**, *113*, 33–44.
- [27] A. Medina-Castillo, J. Fernandez-Sanchez, C. Klein, *Analyst* **2007**, *132*, 929–936.
- [28] S. M. Borisov, I. Klimant, *Anal. Chem.* **2007**, *79*, 7501–7590.
- [29] G. Di Marco, M. Lanza, M. Pieruccini, S. Campagna, *Adv. Mater.* **1996**, *8*, 576–580.
- [30] D. Di Marco, M. Lanza, A. Mamo, I. Stefio, C. Di Pietro, G. Romero, S. Campagna, *Anal. Chem.* **1998**, *70*, 5019–5023.
- [31] L. Huynh, J. Wang, V. Stoeva, A. Lough, I. Manners, M. A. Winnik, *Chem. Mater.* **2005**, *17*, 4765–4773.
- [32] E. Holder, B. M. W. Langeveld, U. S. Schubert, *Adv. Mater.* **2005**, *17*, 1109–1121.
- [33] N. Tian, A. Thiessen, R. Schiewek, O. J. Schmitz, D. Hertel, K. Meerholz, E. Holder, *J. Org. Chem.* **2009**, *74*, 2718–2725.
- [34] N. Rehmann, C. Ulbricht, A. Köhnen, P. Zacharias, M. C. Gather, D. Hertel, E. Holder, K. Meerholz, U. S. Schubert, *Adv. Mater.* **2008**, *20*, 129–133.
- [35] J. F. Fernandez-Sanchez, T. Roth, R. Cannas, Md. K. Nazeeruddin, S. Spichiger, M. Graetzel, U. E. Spichiger-Keller, *Talanta* **2007**, *71*, 242–250.
- [36] J. Brandrup, E. H. Immergut, E. A. Grulke, *Polymer Handbook*, Wiley-VCH, Weinheim, **1999**.
- [37] C. Moore, S. P. Chan, J. N. Demas, B. A. DeGraff, *Appl. Spectrosc.* **2004**, *58*, 603–607.
- [38] M. E. Köse, B. F. Carroll, K. S. Schanze, *Langmuir* **2005**, *21*, 9121–9129.
- [39] G. E. Khalil, C. Costin, J. Crafton, G. Jones, S. Grenoble, M. Gouterman, J. B. Callis, L. R. Dalton, *Sens. Actuators B* **2004**, *97*, 13–21.
- [40] R. Schiewek, M. Lorenz, R. Giese, K. J. Brockmann, T. Benter, S. Gäb, O. J. Schmitz, *Anal. Bioanal. Chem.* **2008**, *392*, 87–96.
- [41] R. Schiewek, M. Schellenträger, R. Mönnikes, M. Lorenz, R. Giese, K. J. Brockmann, S. Gäb, T. Benter, O. J. Schmitz, *Anal. Chem.* **2007**, *79*, 4135–4140.
- [42] S. Lamansky, P. Djurovich, M. E. Thompson, *J. Am. Chem. Soc.* **2001**, *123*, 4304–4312.
- [43] J. I. Kim, I. S. Shin, H. Kim, J. K. Lee, *J. Am. Chem. Soc.* **2005**, *127*, 1614–1615.

Received: June 4, 2009

Published online: September 16, 2009